Revealing Insights into the Axial Coordination Effect of M-N$_4$ Catalysts on Electrocatalytic Activity towards Oxygen Reduction Reaction

Youxuan Ni[1], Weiwei Xie[1]*, Jun Chen[1]*

[1] *Key Laboratory of Advanced Energy Materials Chemistry (Ministry of Education), Haihe Laboratory of Sustainable Chemical Transformations, College of Chemistry, Nankai University, Tianjin 300071, China*

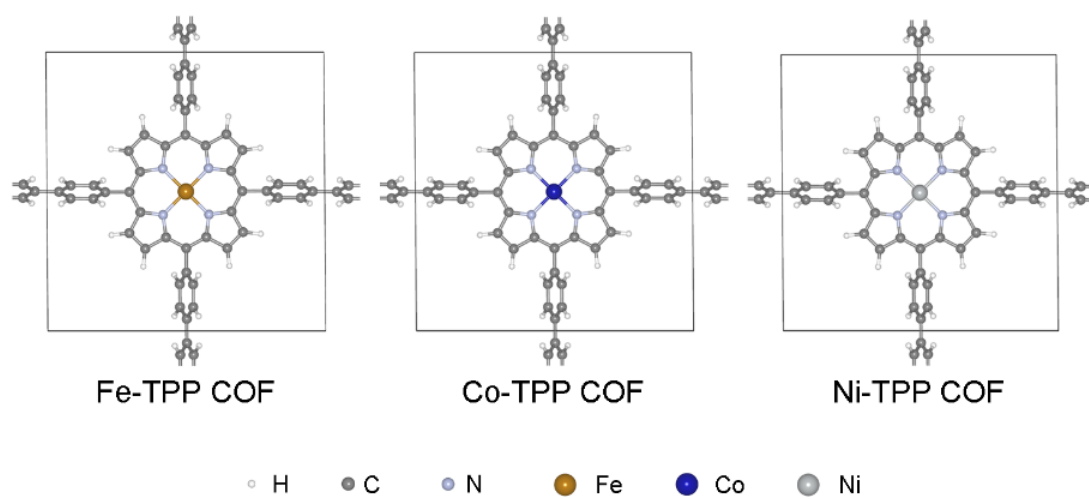Email: xieweiwei@nankai.edu.cn; chenabc@nankai.edu.cn

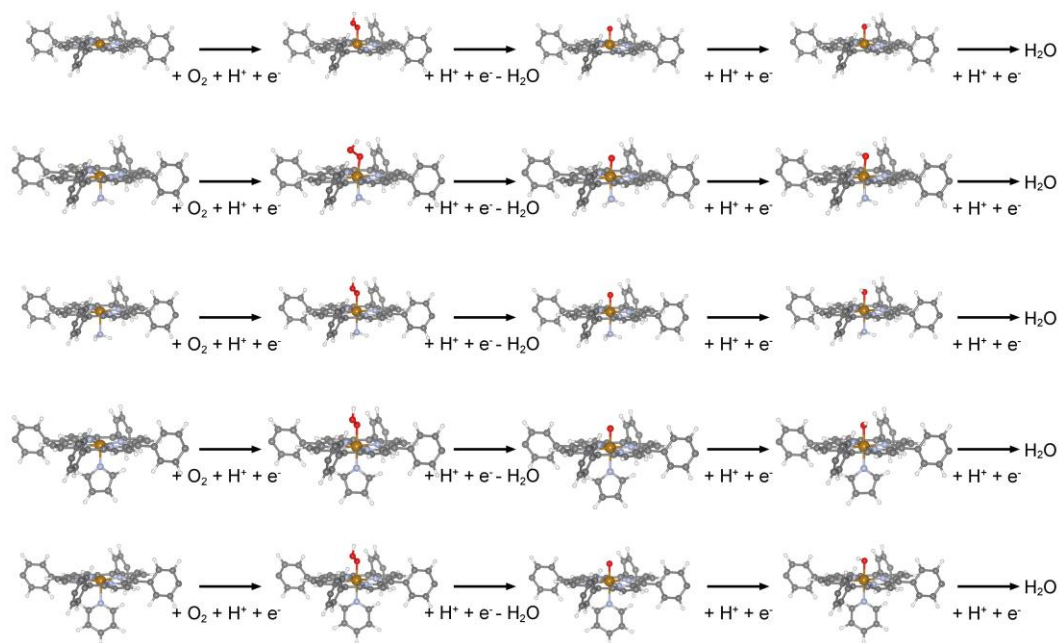Figure S1. The atomic structure of the whole unit cell for the Fe/Co/Ni-TPP COFs.

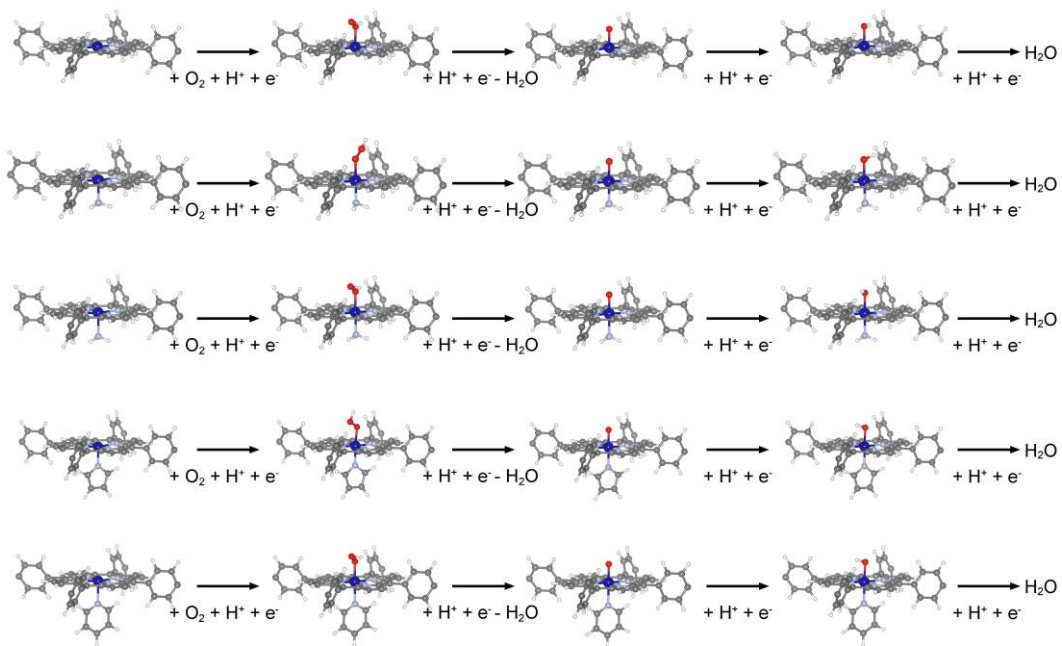Figure S2. ORR routes on Fe-TPP-L COFs (L = none/NH$_2$/NH$_3$/prN/pdN).

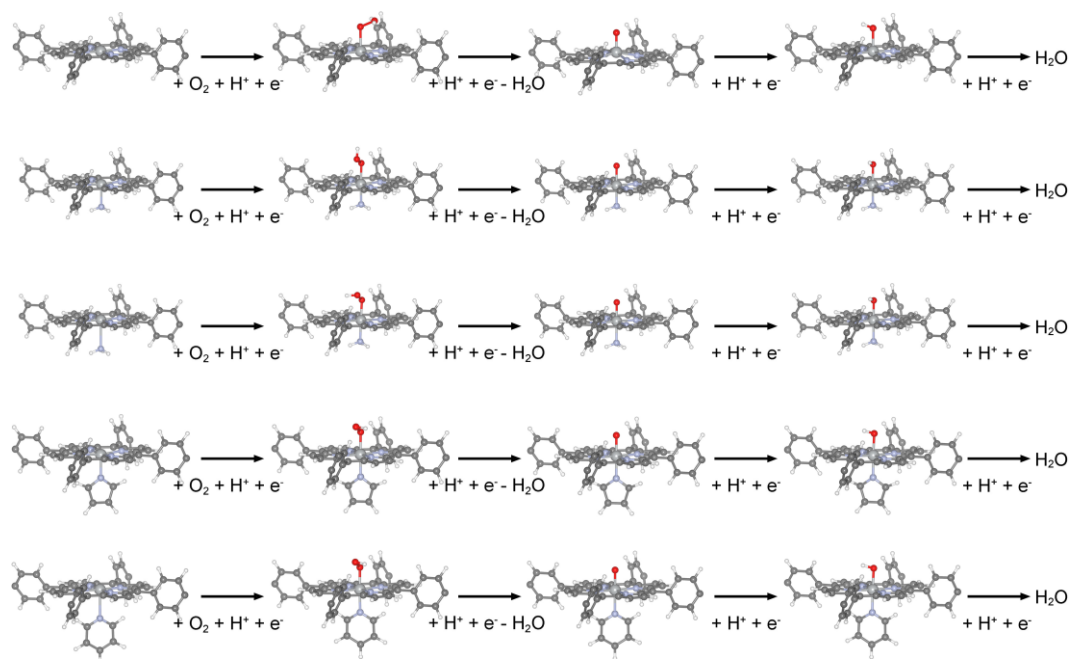Figure S3. ORR routes on Co-TPP-L COFs (L = none/NH$_2$/NH$_3$/prN/pdN).

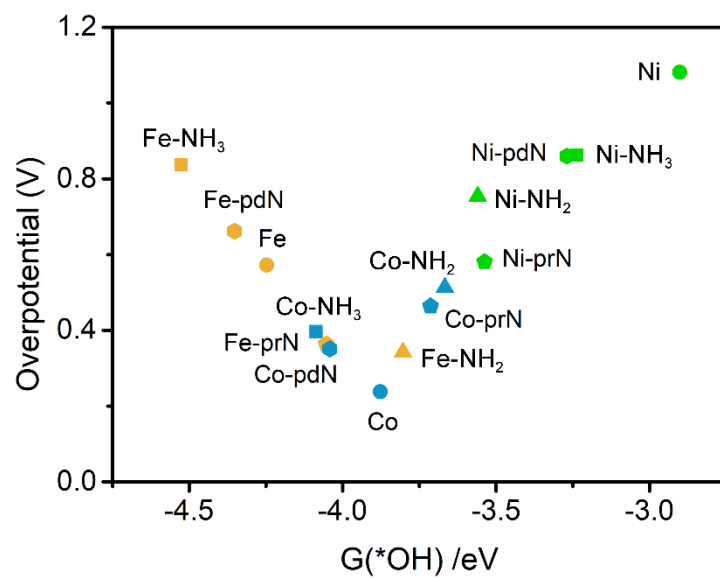Figure S4. ORR routes on Ni-TPP-L COFs (L = none/NH_2/NH_3/prN/pdN).

Figure S5. ORR activity volcano of M-TPP-L COF catalysts (M = Fe/Co/Ni, L = none/NH$_2$/NH$_3$/prN/pdN).
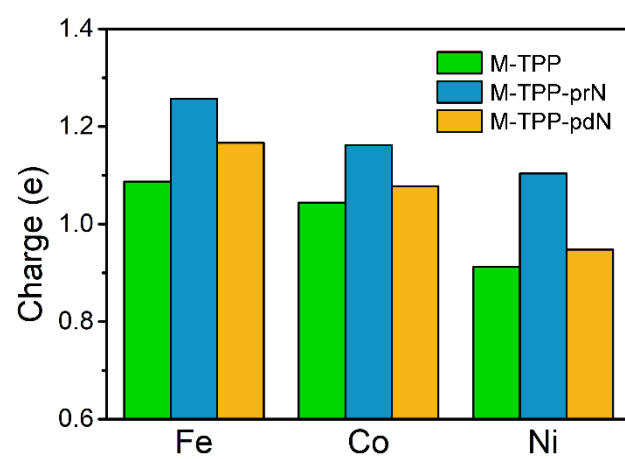
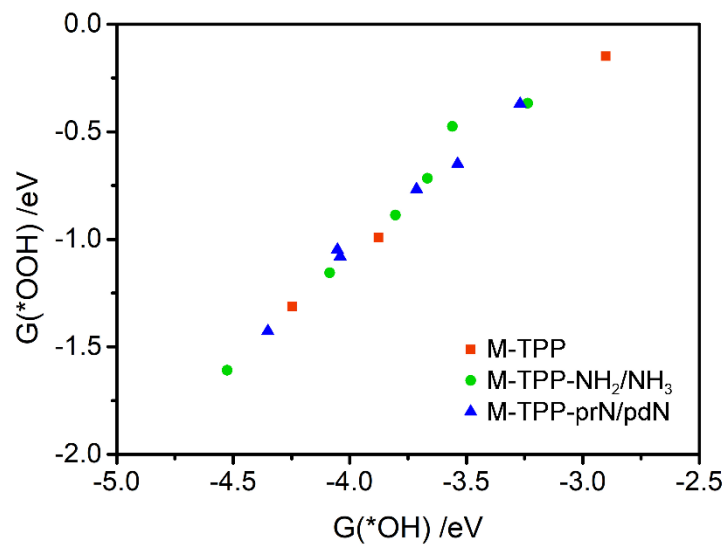Figure S6. Bader charge of Fe, Co and Ni centers on M-TPP-none/prN/pdN COFs.

Figure S7. Linear relationship between Gibbs adsorption free energies of *OOH and *OH for M-TPP-L COF catalysts (M = Fe/Co/Ni, L = none/NH$_2$/NH$_3$/prN/pdN).
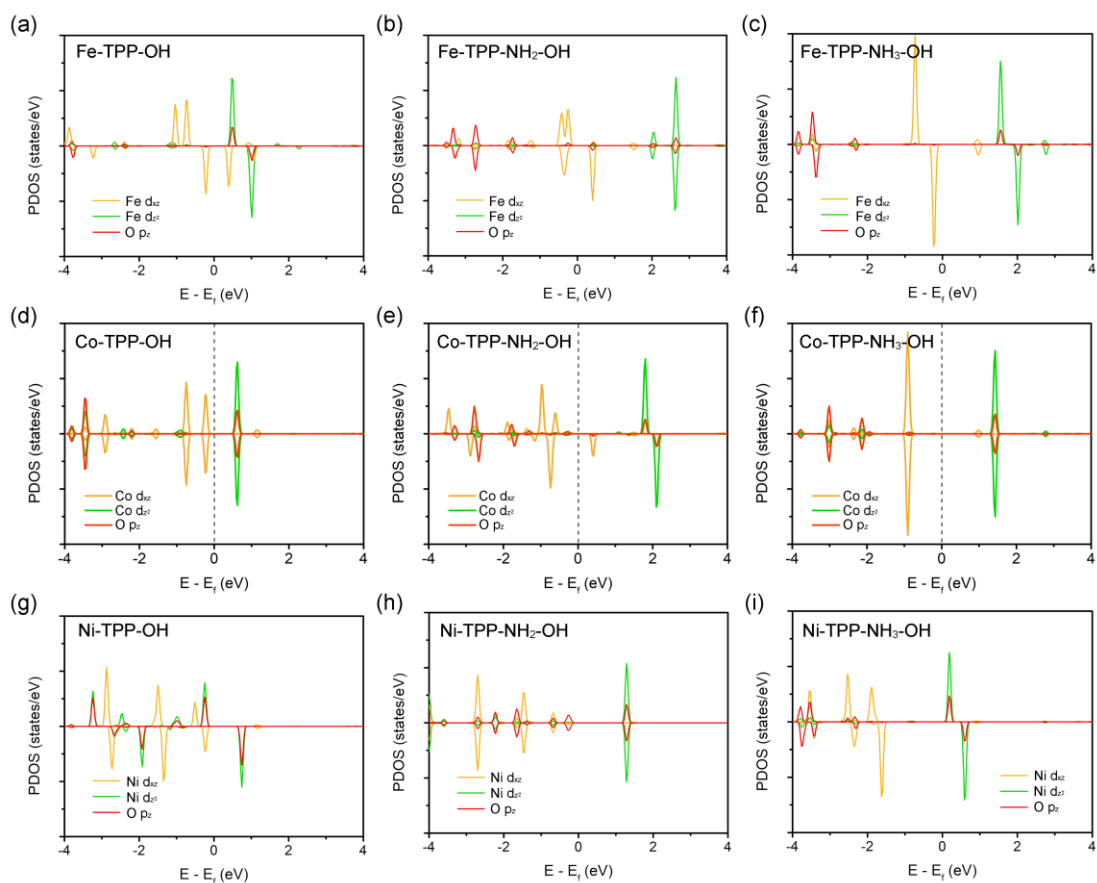
Figure S8. PDOS of (a) Fe-TPP, (b) Fe-TPP-NH$_2$, (c) Fe-TPP-NH$_3$, (d) Co-TPP, (e) Co-TPP-NH$_2$, (f) Co-TPP-NH$_3$, (g) Ni-TPP, (h) Ni-TPP-NH$_2$ and (i) Ni-TPP-NH$_3$ COFs with adsorbed OH species.
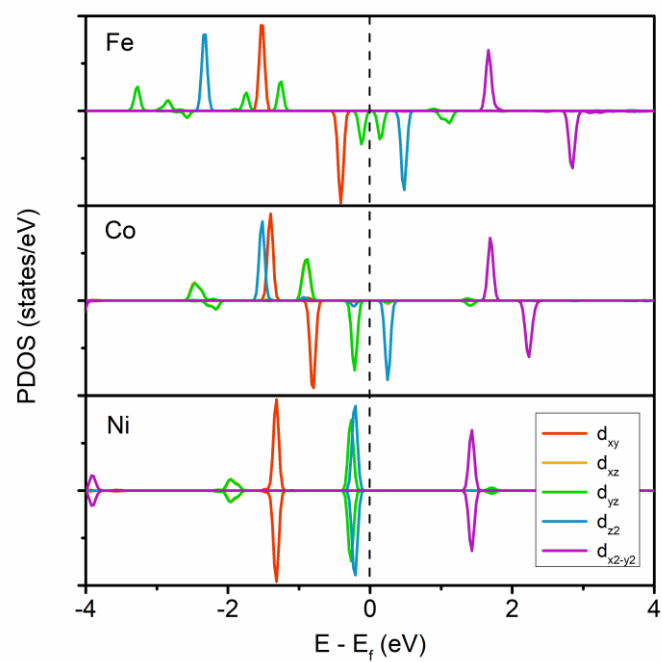
Figure S9. PDOS of d orbitals of Fe, Co and Ni centers in M-TPP COFs without axial ligands.
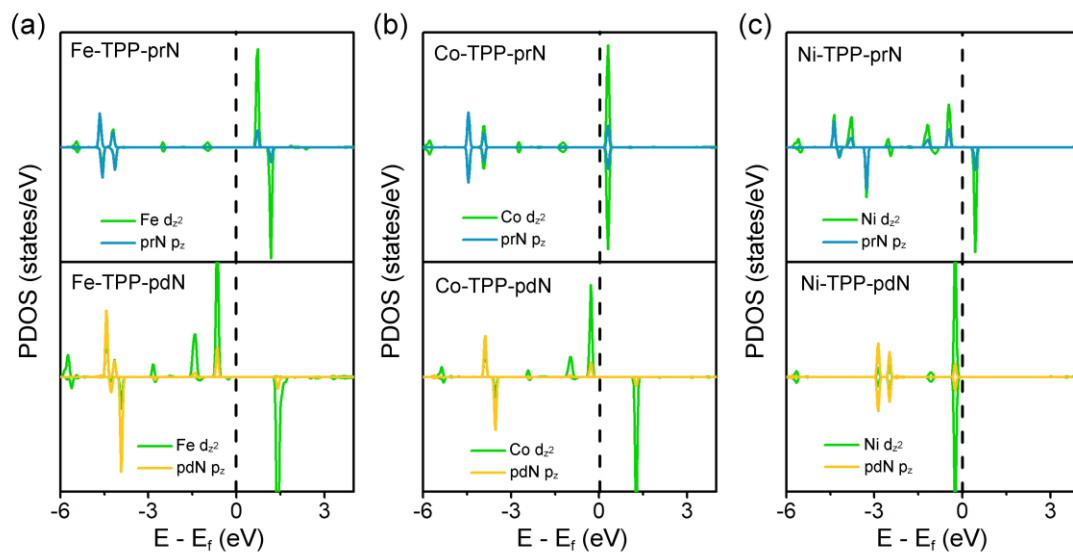
Figure S10. PDOS of (a) Fe-TPP-prN/pdN COFs, (b) Co-TPP-prN/pdN COFs, (c) Ni-TPP-prN/pdN COFs.
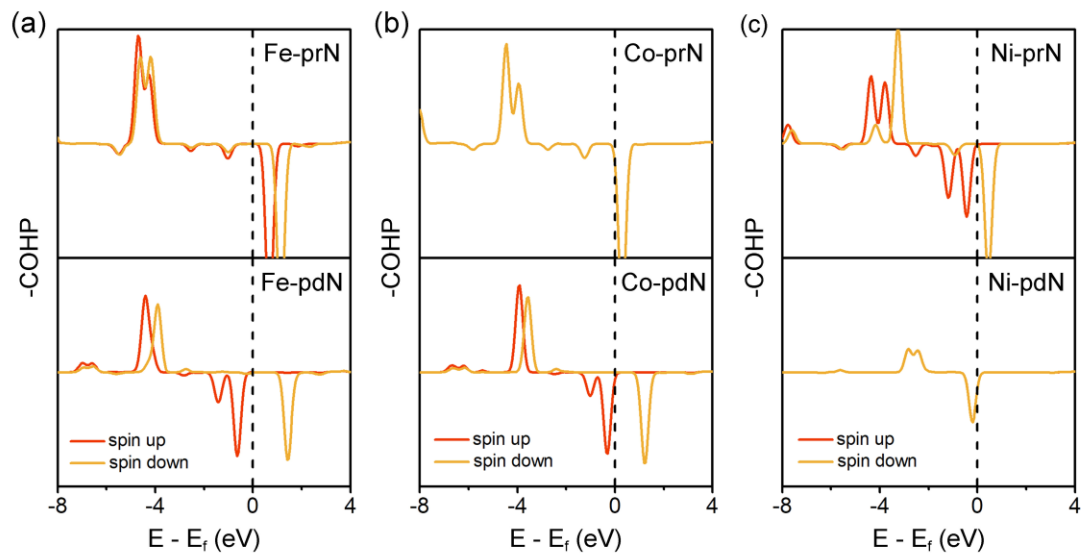
Figure S11. COHP of (a) Fe-TPP-prN/pdN COFs, (b) Co-TPP-prN/pdN COFs and (c) Ni-TPP-prN/pdN COFs.
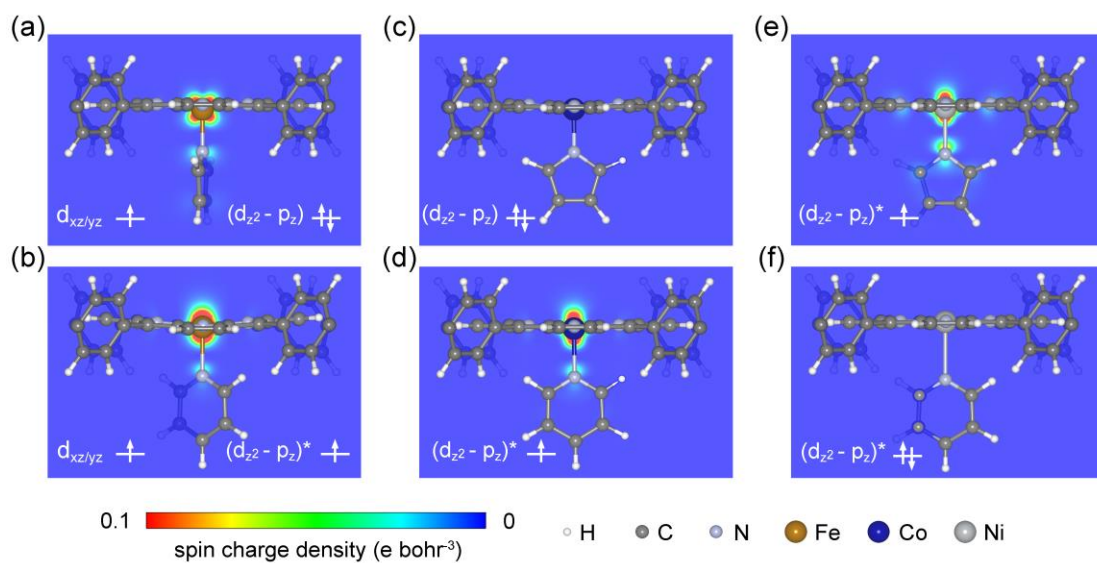
Figure S12. Spin charge density of (a) Fe-TPP-prN COFs, (b) Fe-TPP-pdN COFs, (c) Co-TPP-prN COFs (d) Co-TPP-pdN COFs, (e) Ni-TPP-prN COFs and (f) Ni-TPP-pdN COFs. Spin electrons of catalysts are marked in white.

species	μ (μ_B)	species	μ (μ_B)	species	μ (μ_B)
Fe-TPP	2.00	Co-TPP	1.00	Ni-TPP	0.00
Fe-TPP-OH	1.00	Co-TPP-OH	0.00	Ni-TPP-OH	1.00
Fe-TPP-NH$_2$	1.00	Co-TPP-NH$_2$	0.00	Ni-TPP-NH$_2$	1.00
Fe-TPP-NH$_2$-OH	0.00	Co-TPP-NH$_2$-OH	1.00	Ni-TPP-NH$_2$-OH	0.00
Fe-TPP-NH$_3$	0.00	Co-TPP-NH$_3$	1.00	Ni-TPP-NH$_3$	0.00
Fe-TPP-NH$_3$-OH	1.00	Co-TPP-NH$_3$-OH	0.00	Ni-TPP-NH$_3$-OH	1.00
Fe-TPP-prN	1.00	Co-TPP-prN	0.00	Ni-TPP-prN	1.00
Fe-TPP-prN-OH	2.00	Co-TPP-prN-OH	0.99	Ni-TPP-prN-OH	0.00
Fe-TPP-pdN	0.00	Co-TPP-pdN	1.00	Ni-TPP-pdN	0.00
Fe-TPP-pdN-OH	1.00	Co-TPP-pdN-OH	0.00	Ni-TPP-pdN-OH	1.00

Table S1. The calculated magnetic moments of Fe/Co/Ni-TPP-none/NH$_2$/NH$_3$/prN/pdN COFs and the corresponding systems with adsorbed OH species.
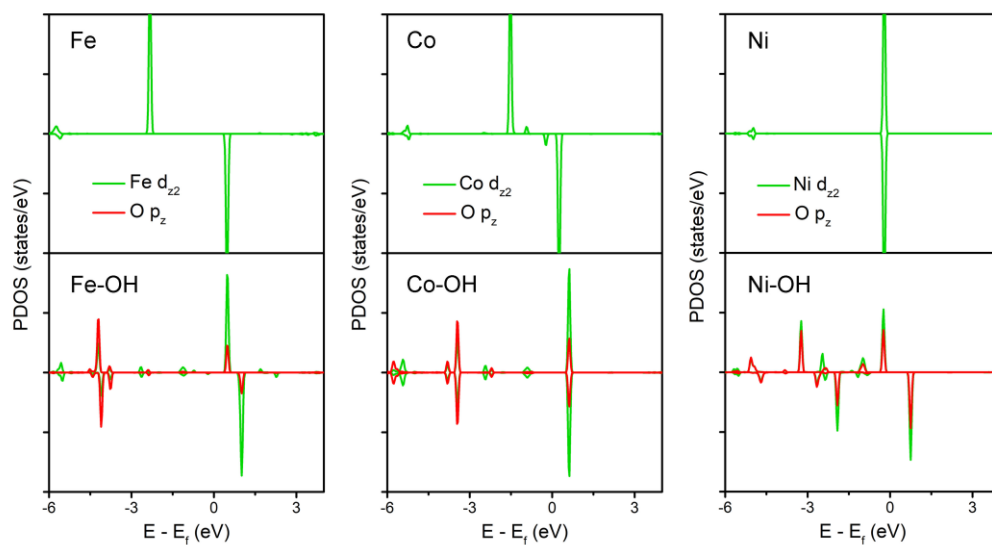
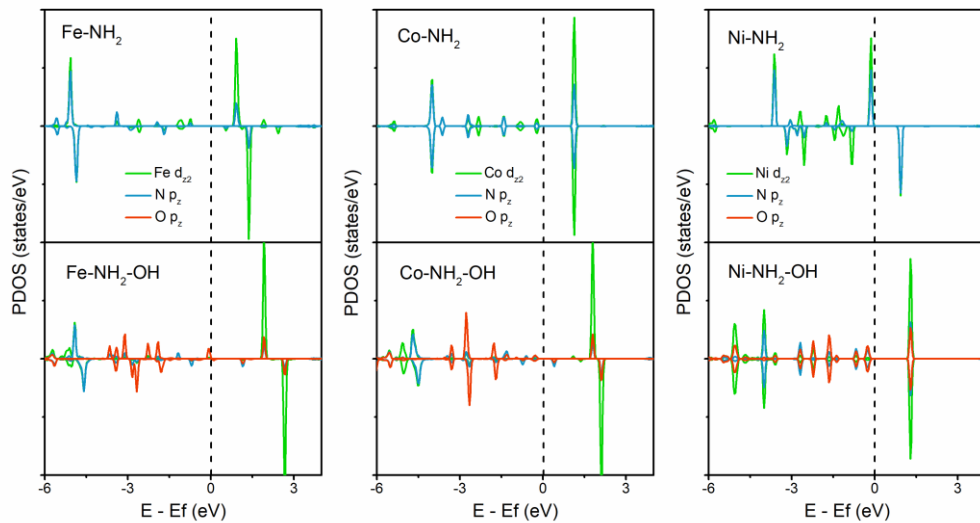Figure S13. PDOS of Fe/Co/Ni-TPP COFs with and without adsorbed OH.

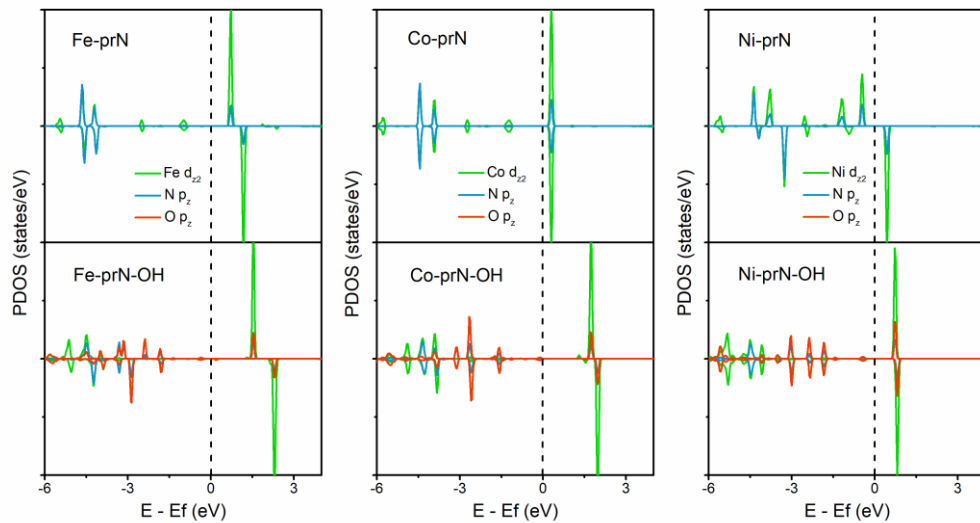Figure S14. PDOS of Fe/Co/Ni-TPP-NH$_2$ COFs with and without adsorbed OH.

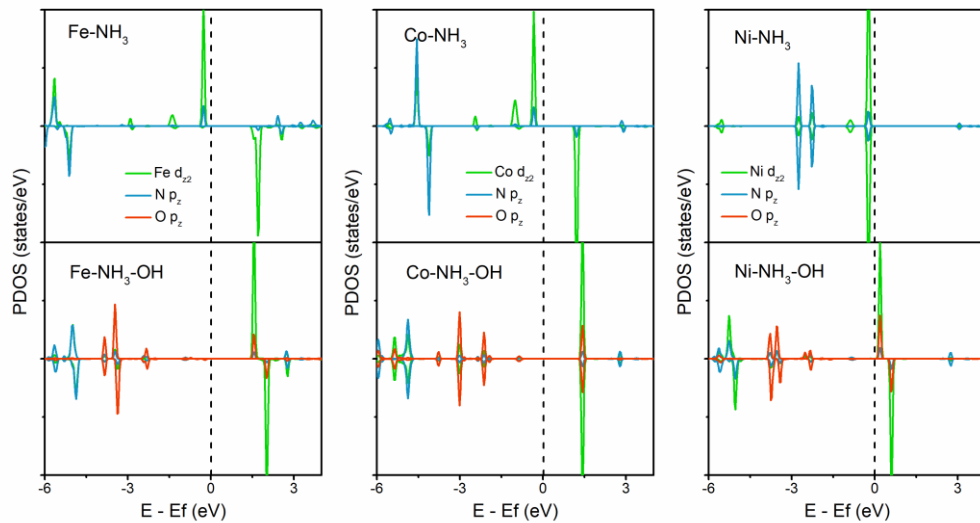Figure S15. PDOS of Fe/Co/Ni-TPP-prN COFs with and without adsorbed OH.

Figure S16. PDOS of Fe/Co/Ni-TPP-NH$_3$ COFs with and without adsorbed OH.
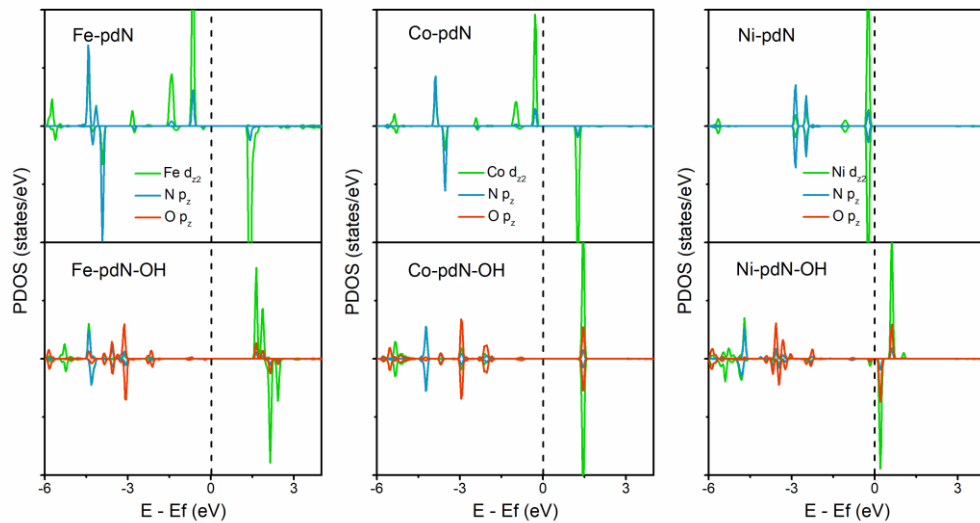
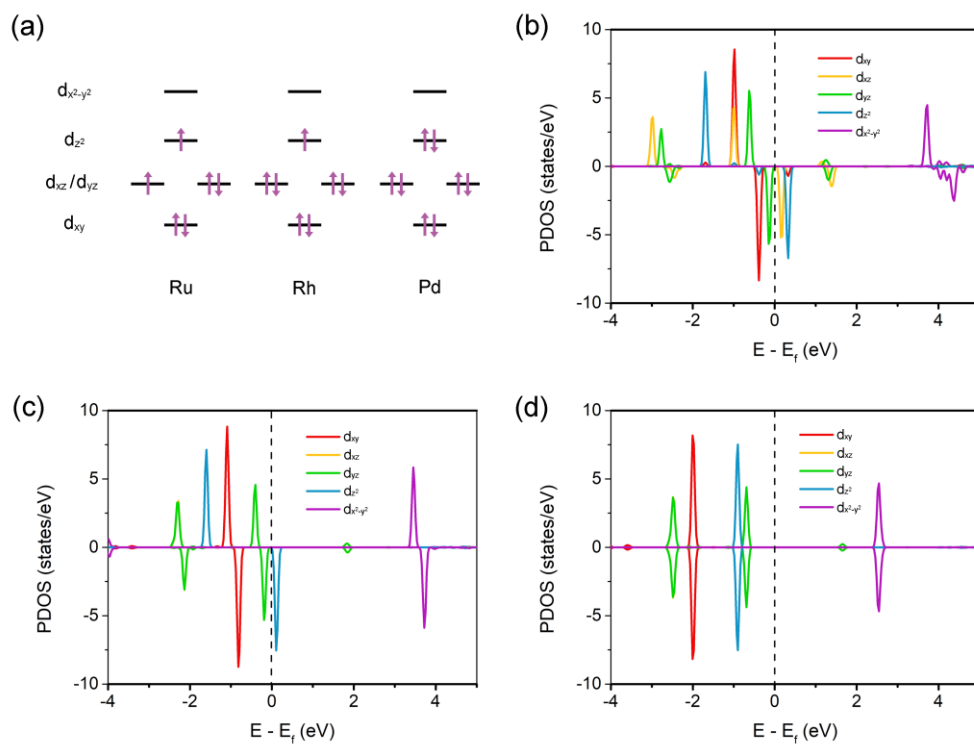Figure S17. PDOS of Fe/Co/Ni-TPP-pdN COFs with and without adsorbed OH.

Figure S18. (a) The d orbitals of metal centers in Ru/Rh/Pd-TPP COFs. The corresponding PDOS of (b) Ru-TPP COFs, (c) Rh-TPP COFs and (d) Pd-TPP COFs.
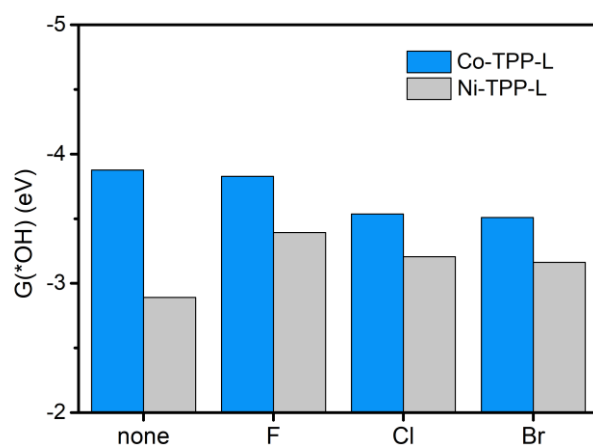
Figure S19. Free energies of *OH intermediates on Co/Ni-TPP-L (L = none/F/Cl/Br).